Out-of-plane Characterization of Silicon-on-insulator Multiuser MEMS Processes-based Tri-axis Accelerometer

[1] Sujatha L., [1] Kalaiselvi S. and [2] Vigneswaran N.

[1] Centre for MEMS & Microfluidics, Rajalakshmi Engineering College, Chennai – 602105 India
[2] Faculty of Electrical and Electronics Engineering, University Malaysia Pahang, Pekan Malaysia
[1] Tel.: 044-37181044, fax: 04437181113
[1] E-mail: sujatha.l@rajalakshmi.edu.in

Abstract: In this paper, we discuss the analysis of out-of-plane characterization of a capacitive tri-axis accelerometer fabricated using SOI MUMPS (Silicon-on Insulator Multi user MEMS Processes) process flow and the results are compared with simulated results. The device is designed with wide operational 3 dB bandwidth suitable for measuring vibrations in industrial applications. The wide operating range is obtained by optimizing serpentine flexures at the four corners of the proof mass. The accelerometer structure was simulated using COMSOL Multiphysics and the displacement sensitivity was observed as 1.2978 nm/g along z-axis. The simulated resonant frequency of the device was found to be 13 kHz along z axis. The dynamic characterization of the fabricated tri-axis accelerometer produces the out-of-plane vibration mode frequency as 13 kHz which is same as the simulated result obtained in z-axis.

1. Introduction

Accelerometers are widely used in industry for measuring vibration in rotating machinery, moving vehicles, aircraft, and in mechanical or civil structures [1] etc., Conventional instruments use piezoelectric technology to monitor the health of the machine for maintenance and safety. Although piezoelectric based device is well matured, MEMS based devices are gaining increased attention due to their several advantages [2] such as smaller size (in micro meter), very low mass, scope for mass production, low cost, robustness and reliability, repeatability, temperature insensitivity through suitable compensation and microelectronic fabrication process compatibility which enables ease of integration. The wide operating bandwidth and increased sensitivity of tri-axis accelerometer offer wide range of applications in industries for monitoring vibrations in rotating machines.

The various transduction principles like piezoelectric, piezo resistive, thermal, resonant and capacitive are commonly used in MEMS accelerometer. Piezo-electric accelerometers are based on piezo materials that produce electric charge proportional to applied force [3-4]. The Piezo-resistive accelerometer uses silicon strain gauges in a bridge configuration [5-7]. These devices are capable of measuring static acceleration. The thermal accelerometer measures the temperature difference proportional to acceleration [8]. The capacitive accelerometer [9-14] converts mechanical movement of a proof mass to proportional capacitance change. Capacitive accelerometers have several advantages like high sensitivity, capability to measure static states as well as dynamic changes, low power consumption and temperature stability through suitable compensation.

The tri-axis MEMS accelerometer has also been frequently used to detect displacement, acceleration

and velocity in the industrial applications for monitoring vibrations [15]. The tri-axis accelerometer based on capacitive type has been reported by many researchers. The sensing comb drives are distributed along the edges of the proof mass and supporting structure. The proof mass of dimension 700 μm x 700 μm as described in [16] suffers from unwanted pre deformation due to its large suspension structure which reduces the sensitivity of the device. The multilayer metal with stacked dielectric vertically integrated with fully differential electrodes in in-plane and out-of-plane reduces the foot print of the accelerometer with increased sensitivity and reduced noise [17]. The POLY MUMPS fabricated three individual axis accelerometers integrated on single substrate to produce low mechanical noise and high sensitivity has been reported [18]. A distinct measurement system of three-axis micro-accelerometer to measure the noise and reliability has been reported [19].

The SOI based capacitive accelerometer has been reported by many people. The in-plane capacitive accelerometer with compliant amplifiers fabricated using SOI MUMPS enhances both sensitivity and bandwidth [20]. The out-of-plane accelerometer with asymmetrical sensing comb drives used for high aspect ratio structures was fabricated by SOI process [21]. The decoupled frames supported by spring and capacitive compensator helps in achieving low cross-axis sensitivity [22]. The optimized design for high resolution of single axis accelerometer was fabricated by SOI process [12]. The advantages of SOI based device are excellent mechanical property of structural layer, possibility of fabricating high aspect ratio structures using DRIE (deep reactive ion etching), good electrical isolation between the structural and substrate silicon by oxide layer, enabling ease of integration with electronics. Thus SOI technology provides a great opportunity for high performance MEMS device.

This paper presents the design, fabrication and out-of-plane characterization of MEMS tri-axis accelerometer fabricated by SOI technology with wide operating 3dB bandwidth. The serpentine flexures are designed for sensing acceleration in in-plane and out-of-plane direction.

2. Design

The tri axis accelerometer is modelled as a mass spring damper system [23] as show in Fig. 1. The equation governing the second order is given by

$$m\ddot{x} + c\dot{x} + kx = -F = -ma, \tag{1}$$

where m is the mass of the proof-mass, x is the displacement of the proof-mass, c is the damping coefficient, k is the spring constant, F is the applied force and a is the acceleration.
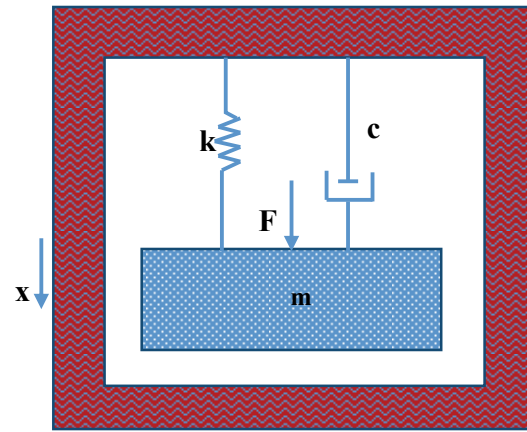

Fig. 1. Mass spring damper system.

In the static response the accelerometer is excited with acceleration of amplitude 'a' and frequency 'ω'=0. The amplitude of the response is given by

$$x = -\frac{m}{k}\, a \tag{2}$$

the displacement sensitivity is given as

$$S_d = \frac{m}{k} = \frac{x}{a}, \tag{3}$$

where S_d is the displacement sensitivity of the accelerometer defined as the ratio of displacement of the proof mass to unit gravitational acceleration.

The dynamic response of the accelerometer is obtained by taking Laplace transform to the equation (1)

$$\frac{X(s)}{F(s)} = \frac{1}{ms^2 + cs + k} \tag{4}$$

$$\frac{X(s)}{F(s)} = \frac{1/m}{s^2 + 2\xi\omega_n s + \omega_n^2 k} \tag{5}$$

where the ω_n is the natural frequency

$$\omega_n = \sqrt{\frac{k}{m}} \tag{6}$$

where ξ is the damping ratio term

$$\xi = \frac{c}{2\sqrt{km}} = \frac{c}{c_r} \tag{7}$$

where c_r is the critical damping coefficient

$$c_r = \sqrt{km} \tag{8}$$

Under sinusoidal input

$$f(t) = F\sin\omega t = ma\sin\omega t \tag{9}$$

The steady state response will be sinusoidal signal with same frequency is

$$x = A \sin(\omega t + \varphi) \qquad (10)$$

therefore, the magnitude A is

$$A = \frac{F/m}{\sqrt{(\omega_n^2 - \omega^2)^2 + 4\xi^2 \omega^2 \omega_n^2}} \qquad (11)$$

The phase φ is $\quad \varphi = e^{in\theta} = \frac{2\xi\omega\omega_n}{(\omega_n^2 - \omega^2)^2} \qquad (12)$

The device is operated at a low frequency than the resonant frequency i.e., $\omega <<< \omega_n$

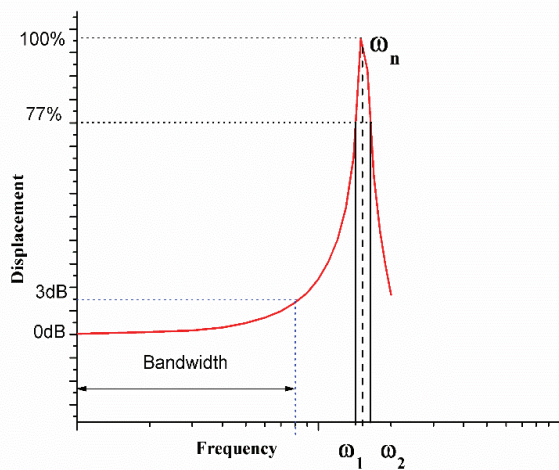Hence, $A = \frac{F/m}{\omega_n} = \frac{a}{\omega_n^2} \qquad (13)$

Fig. 2. Typical frequency response of accelerometer.

The amplitude of displacement remains constant for certain range of frequency. The response from zero to the frequency corresponding to 3 dB gain is known as bandwidth of the device. When we operate the device at resonant frequency the amplitude reaches maximum displacement of $1/2\xi$ and phase difference of 90° between applied force and obtained displacement. The resonance may increase the sensitivity however, may lead to damage to mechanical device. At a frequency less than resonant frequency the amplitude of displacement decreases. The Quality factor represents to sharpness of the resonance peak which is defined by

$$Q = \frac{\omega_n}{\Delta\omega} = \frac{1}{2\xi} = \frac{\omega_n}{\omega_2 - \omega_1} \qquad (14)$$

The quality factor is inversely proportional to the damping factor. The quality factor is the ratio of resonant frequency (ω_n) to spacing between the two frequency (ω_1 and ω_2) at half power.

A typical frequency response of an accelerometer is shown in Fig. 2. From the expressions (3) and (6), it is clear that sensitivity is directly proportional to the mass and inversely proportional to the spring constant. But, the natural frequency of the flexure is directly proportional to spring constant and inversely proportional to mass. So, to design a high bandwidth and improved sensitivity optimal value of mass and stiffness must be selected. But, high mass in-turn reduces the natural frequency of the system. So, to design a high bandwidth device, the stiffness has to be very high keeping mass at an optimal value.

The MEMS tri- axis capacitive accelerometer consists of proof mass with interdigitated sensing fingers which is suspended by four serpentine flexures as shown in Fig 3. The fixed finger is attached to the electrode to form the differential capacitance. When the accelerometer is subjected to change in acceleration in any arbitrary direction, the movement of the proof mass causes the flexures to deform which results in change of differential capacitance. This change in capacitance can be detected by the interface circuit whose output voltage gives the measure of applied acceleration. This enables the accelerometer to detect the motion.
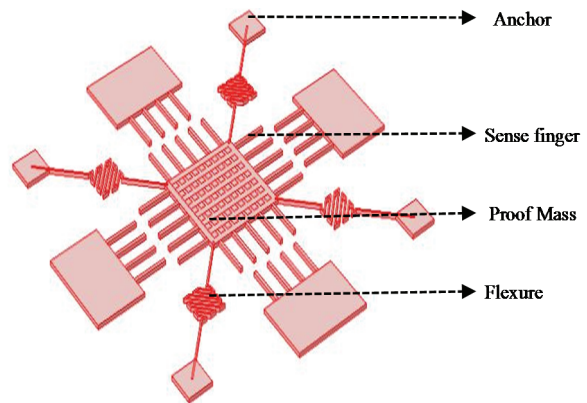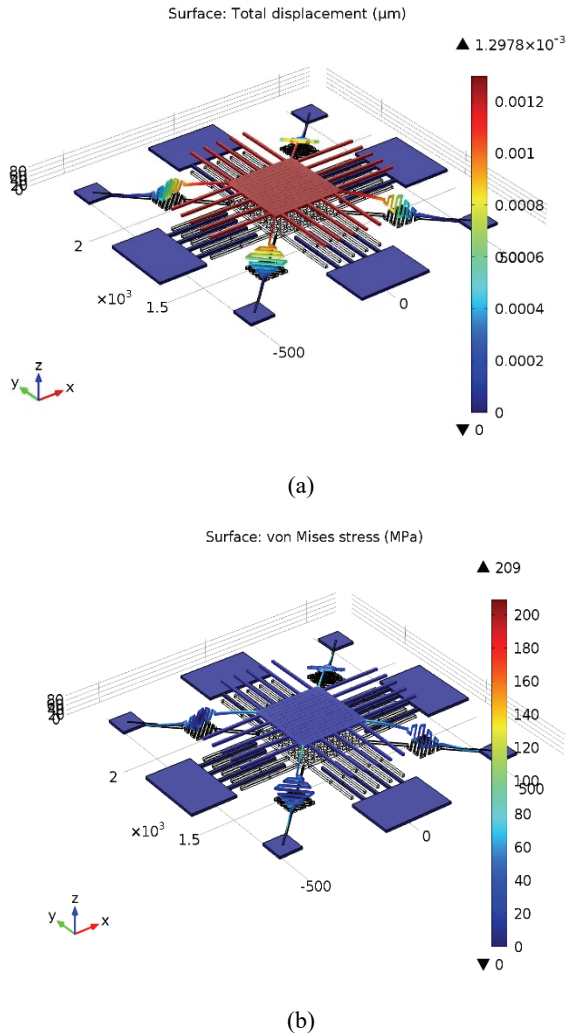

Fig. 3. 3D Schematic diagram of Tri axes accelerometer.

2.1. Finite Element Analysis of Tri Axis Accelerometer

The sensor has an overall dimension of approximately 1.5 mm × 1.5 mm in footprint, with a structural thickness of approximately 10 μm. The designed accelerometer consists of a 300 μm × 300 μm proof mass, 32 pairs of sensing comb drives, and four serpentine flexures through which the proof mass is anchored to the substrate. The dimension of each comb drive is 130 μm x 10 μm. The equivalent dimension of each serpentine flexure is 424 μm × 5 μm. The performance of the accelerometer depends on the flexure which provides the mechanical displacement. To achieve higher bandwidth, the tri axis accelerometer serpentine flexure are designed as shown in Fig 3. Simulations were carried out to find the behaviour of the tri axis accelerometer using COMSOL Multiphysics.

2.1.1. Static Analysis

The 3D parametric static analysis was performed by applying body force from 1 g to 10 g along x, y and z axes. The displacement profile along z axis is shown in Fig. 4 (a). The stress distribution of out-of-plane axis under acceleration of 500 g is shown in Fig. 4 (b).
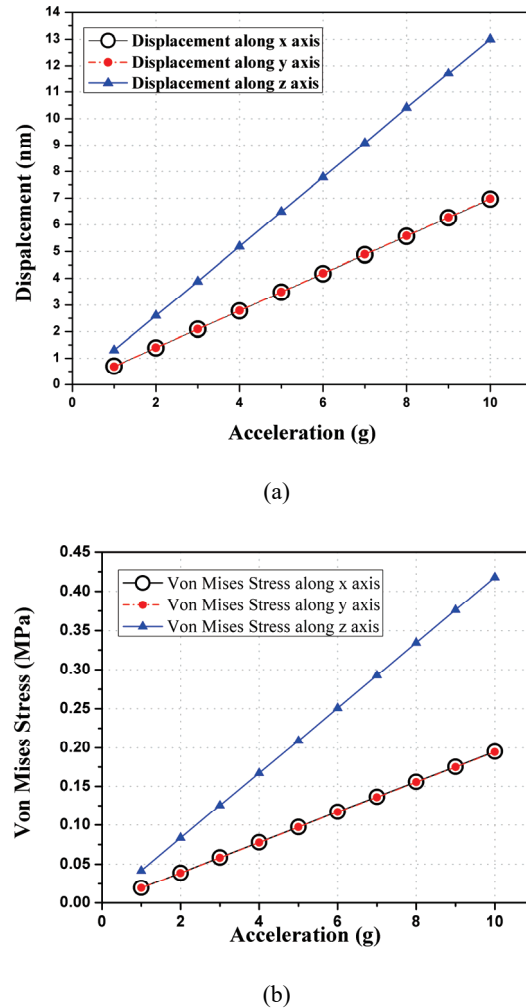
acceleration. The sensitivities obtained were 0.6957 nm/g, 0.6981 nm/g and 1.2978 nm/g along x, y and z axes respectively. The stress versus acceleration plot is as shown in Fig. 5 (b) for the acceleration from 1 – 10 g. The symmetrical geometry along x and y axes results in identical sensitivity and stress distribution for a given acceleration.

(a)

(a)

(b)

Fig. 4. (a) Displacement along out-of-plane mode, (b) Stress distribution along out-of-plane mode.

(b)

Fig. 5. (a) Displacement as a function of acceleration (b) Von Mises stress as a function of acceleration.

It is also found that the device shows a maximum stress of 97 MPa and 209 MPa along in-plane and out-of-plane axis respectively under 500 g static load which is well within the yield strength of silicon. The displacement versus acceleration was plotted for different values of g as shown in Fig. 5(a). The displacement versus acceleration is observed to be very much linear.

The proof mass shows a deflection of 6.957 nm, 6.9807 nm and 0.013 µm under 10 g along x, y and z axes respectively as shown in Fig. 5 (a). The displacement sensitivity was measured by calculating the slope for different values of displacement and

2.1.2. Eigen Frequency Analysis and Frequency Response

COMSOL Multiphysics has the capability of performing the Eigen frequency analysis. The first two in-plane modal resonant frequencies were found to be 19.206 kHz and 19.177 kHz in x and y axes is shown in Figs. 6 (a) and (b). The first out-of-plane modal resonant frequency was found to be 14.064 kHz is shown in Fig. 6 (c). Presence of symmetrical flexure design along x and y axis produces the same modal frequency. The other Eigen frequencies in the out-of-plane mode are shown in Fig. 7.
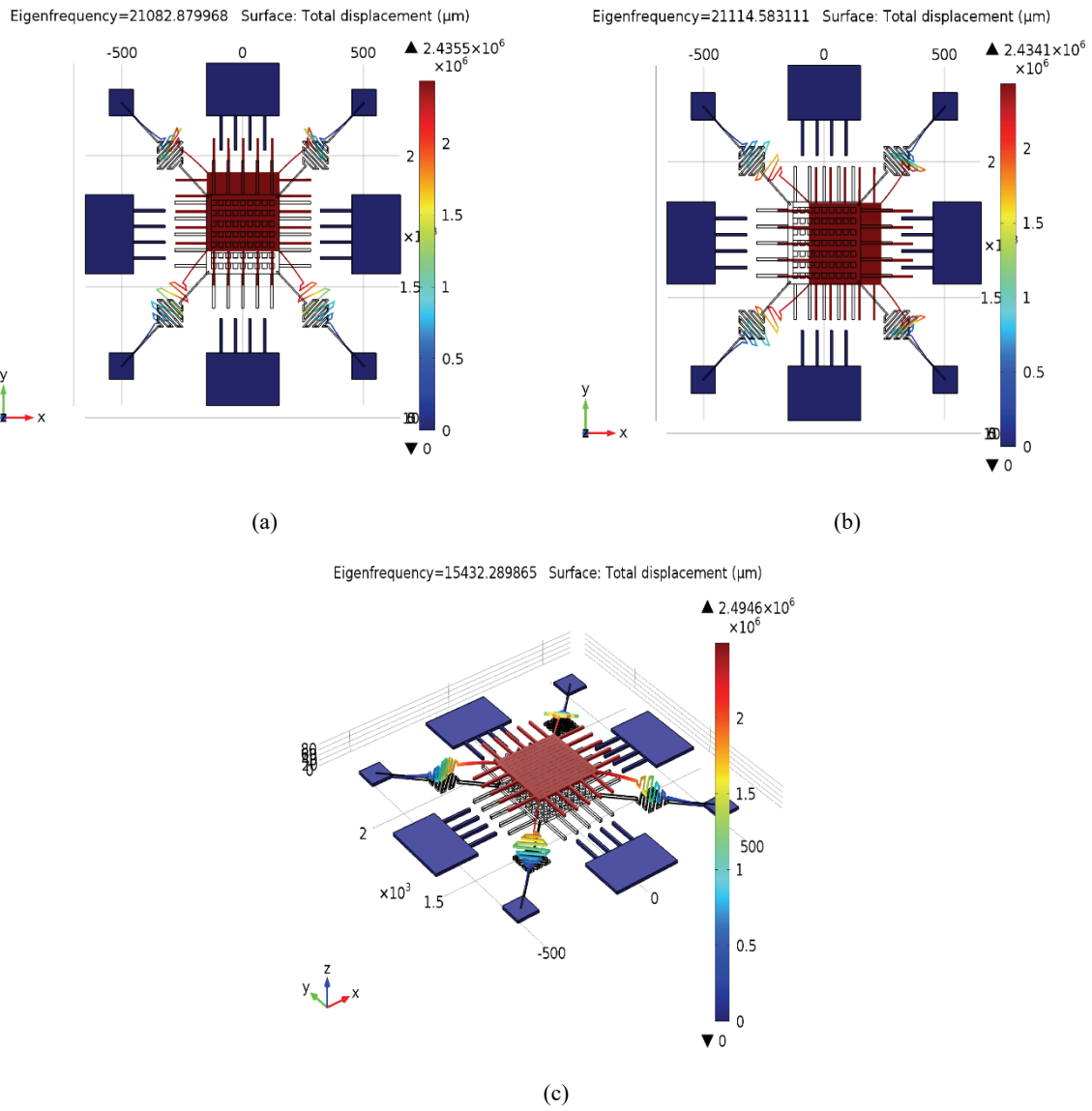
(a)   (b)

(c)

Fig. 6. Simulated (a) First in-plane modes of vibration in x axis; (b) First in-plane modes of vibration in y axis; (c) First out-plane modes of vibration in z axis.
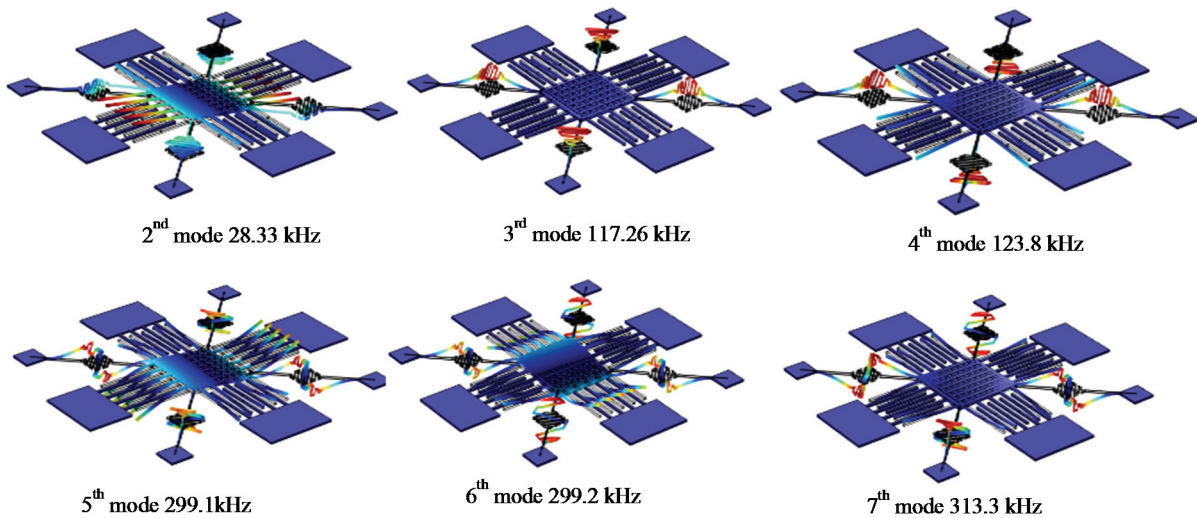

2nd mode 28.33 kHz   3rd mode 117.26 kHz   4th mode 123.8 kHz

5th mode 299.1kHz   6th mode 299.2 kHz   7th mode 313.3 kHz

Fig. 7. Other Eigen Frequency in out-of-plane mode.

To study the frequency response, the input frequency was swept from 1 kHz to 30 kHz along x and y axes and 1 kHz to 20 kHz along z axis under 1 g acceleration.

The simulated dynamic displacement behavior of the device is shown in Fig. 8(a) and (b), the results shows identical magnitude and phase response along x and y axes. The maximum displacement occurs at its resonant frequency. The magnitude response plot helps to determine the 3 dB operating bandwidth of the in-plane mode which is approximately 10 kHz and the out-of-plane mode is approximately 7 kHz. The 90° phase change was observed at its resonant frequencies along x, y and z axes as shown in the phase response plot. The Quality factor of tri-axis accelerometer along in-plane and out-of-plane mode is found to be approximately 7 and 14 respectively using equation 2.14.
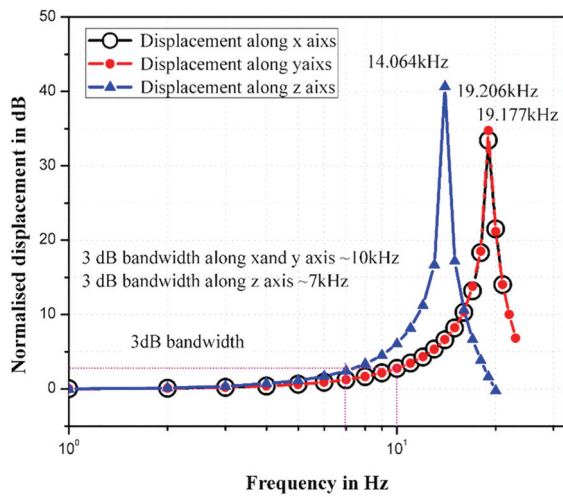

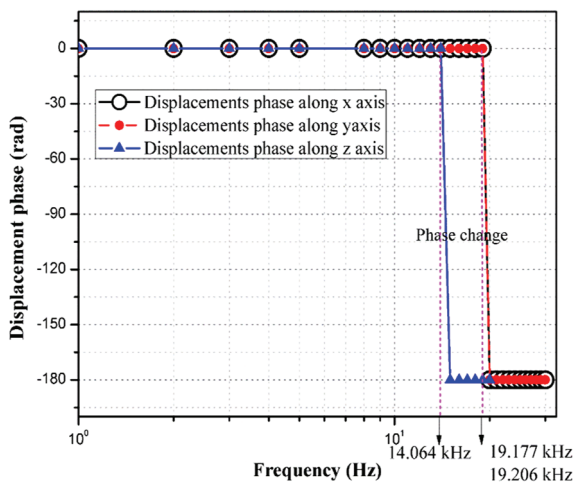**Fig. 8 (a).** Magnitude response of the device.

Fig. 8 (b). Phase response of the device.

The dynamic vibrational behavior of the device was simulated and velocity versus frequency response is shown in Fig. 9. The maximum velocity occurs at 18 kHz and 13 kHz along in-plane and out of plane axis.
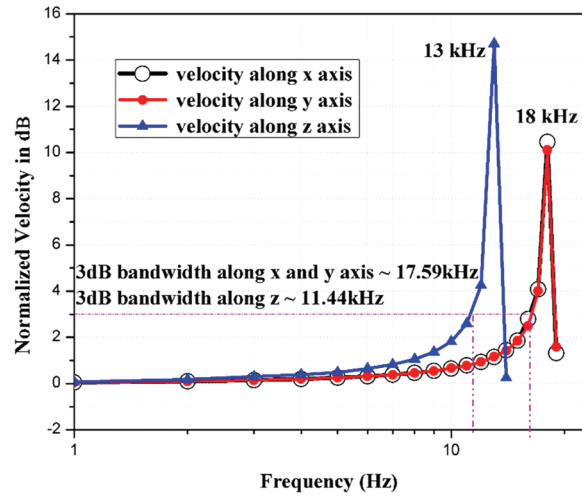

Fig. 9. Velocity and frequency response of the device.

3. Fabrication

The design of three-axis accelerometer was fabricated using SOIMUMPs [24] which is established a micro-system foundry to realize the device. SOIMUMPs use Silicon-on-Insulator wafer with 10 μm thick structural layer, 1 μm thick buried oxide layer and 400 μm thick substrate or handle layer.

The device was made by patterning the 10 μm thick structural layer. The cross sectional view of the structure as shown in the Fig. 10. Fabrication of device requires preparation of Photo masks from the design. The mask layout used in the fabrication of the device as shown in the Fig. 11 were (a) oxide layer mask (negative mask) (b) Silicon device layer with combs and flexures mask and (c) metal contact mask (positive mask). The designed structure follows the process and rules of SOI MUMPS [24]. Optical Microscopy image of the fabricated tri-axis accelerometer are shown in the Fig. 12.
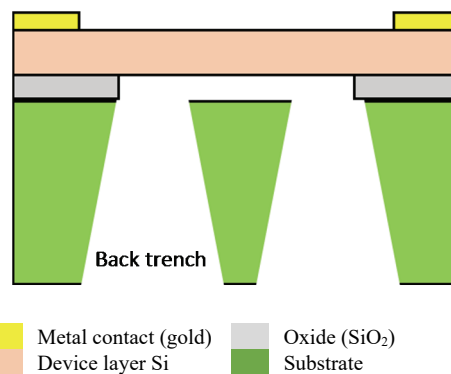

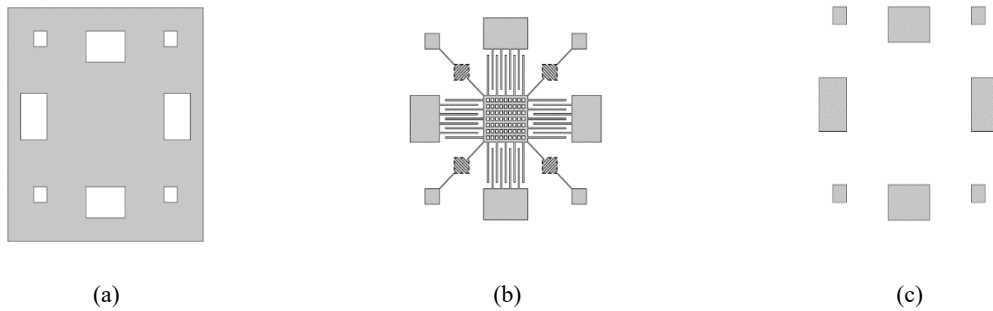**Fig. 10.** Cross sectional view of tri-axis accelerometer.

(a)   (b)   (c)

Fig. 11. Mask layout for (a) Mask 1(oxide – negative mask); (b) Mask 2 (device layer), and (c) Mask 3 (Metal Contact).
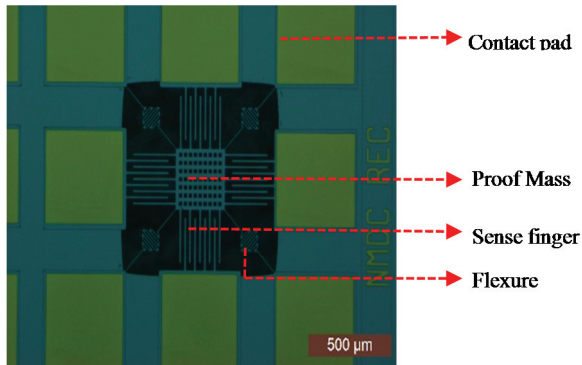

Fig. 12. Optical Microscopy image of released tri axis accelerometer with Contact pad.

4. Results and Discussion

The POLYTEC MSA-400 Micro System Analyzer is used for dynamic analysis and visualization of structural vibrations of fabricated tri-axis accelerometer by fully integrating a microscope with Scanning Laser Doppler Vibrometer and Stroboscopic Video Microscope. The MSA 400 uses Doppler shift mode to measure the out-of-plane vibrations and motions whereas it uses stroboscopic mode to measure the in-plane vibrations and motions [25].

4.1. Out-of-plane Frequency Response for Tri-axis Accelerometer

The device under test was actuated electrostatically using an alternating voltage of above the DC bias of 1 V by probing on the gold contacts pads of the device. The frequency of the applied voltage is swept from 1 kHz to 400 kHz. The Analyzer computes the frequency response and displays the results. The amplitude of vibration velocities at various frequencies were recorded and plotted as shown in Fig. 13.
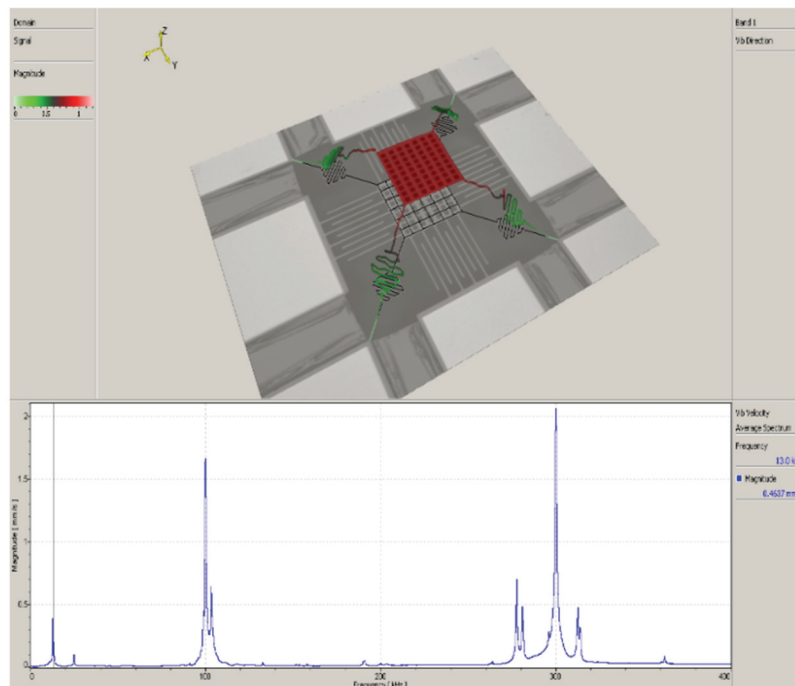

Fig. 13. Out-of-plane displacement at first mode and the frequency response characteristics by MSA 400 (Video 1).

Experimentally obtained first mode out-of-plane resonant frequency was found to be 13 kHz at ambient pressure as shown in Fig. 13 (Video 1). The measured resonant frequency (13 kHz) matches with the simulated result. It should be noted that significant peaks are observed at different modes of frequency such as 24.8 kHz, 100 kHz, 103.3 kHz, 277.8 kHz, 280.9 kHz and 300.3 kHz as shown in Fig. 14 (Video 2 – 7) and these frequencies are closely matching with the corresponding modes obtained by simulation as shown in Fig. 7.
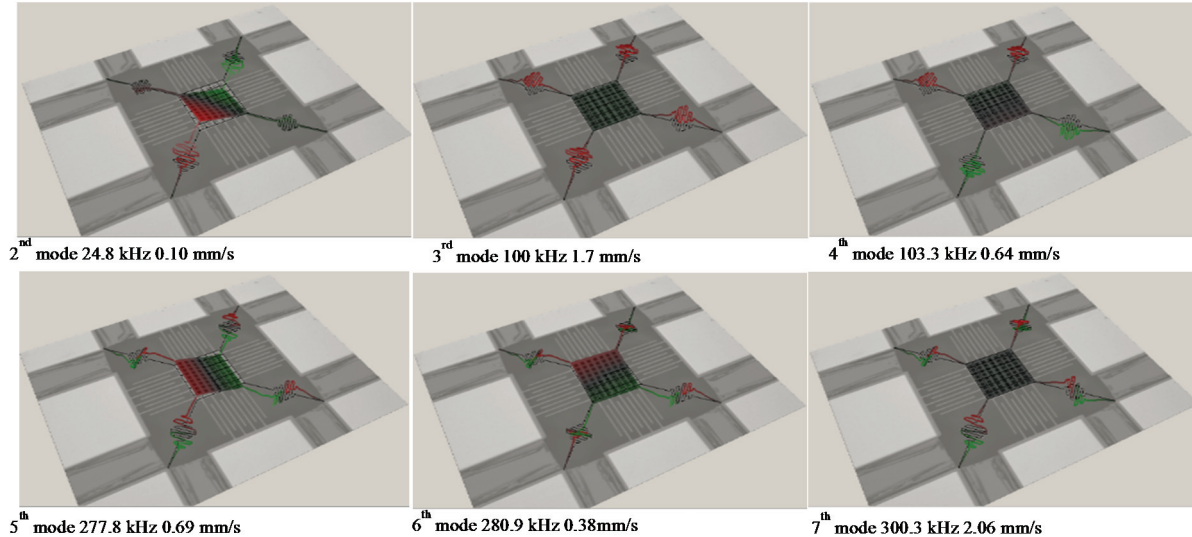

2nd mode 24.8 kHz 0.10 mm/s 　　 3rd mode 100 kHz 1.7 mm/s 　　 4th mode 103.3 kHz 0.64 mm/s

5th mode 277.8 kHz 0.69 mm/s 　　 6th mode 280.9 kHz 0.38mm/s 　　 7th mode 300.3 kHz 2.06 mm/s

Fig. 14. Higher modes of the accelerometer (Video 2 – 7).

5. Conclusion

The analysis of out-of-plane characterization of tri-axis capacitive accelerometer facilitated by SOI MUMPS technology is discussed in this paper.

This work is aimed to provide wide operating 3dB bandwidth suitable for vibration monitoring applications. The device was designed using serpentine flexure which can de-couple any in-plane vibration or out-of- plane vibration into its axial components. Simulations were carried out to find the behavior of the tri-axis accelerometer using COMSOL Multiphysics. Static analysis, stress analysis and Eigen frequency analysis using the simulations were discussed. The simulation results show out-of-plane resonant frequency in z-axis as 13 kHz and the 3 dB operating bandwidth as 11.438 kHz. The fabricated device shows out-of-plane resonant frequency as 13 kHz and also the same 3dB operating bandwidth. The in-plane dynamic characterizations of the device and capacitance measurements are being carried out.

Acknowledgements

References

[1]. Mark Looney, An Introduction to MEMS Vibration Monitoring, *Analog Dialogue*, Vol. 48, 2014, pp. 06.

[2]. Subimal Bikash Chaudhury, Mainak Sengupta and Kaushik Mukherjee, Vibration Monitoring of Rotating Machines Using MEMS Accelerometer, *International Journal of Scientific Engineering and Research*, Vol. 2, Issue 9, 2014, pp. 5-11.

[3]. Alhussein Albarbar et al., Suitability of MEMS Accelerometers for Condition Monitoring: An experimental study, *Sensors,* Vol. 8, 2008, pp. 784-799.

[4]. Zhiyuan Shen et al., A miniaturized wireless accelerometer with micromachined piezoelectric sensing element, *Sensors and Actuators A*, Vol. 241, 2016, pp. 113–119.

[5]. E. Jesper Eklund et al., Single-mask SOI fabrication process linear and angular piezoresistive accelerometers with on-chip reference resistors, *IEEE Sensors*, 2005, pp. 656-659.

[6]. Anindya Lal Roy et al., Design, fabrication and characterization of high performance SOI MEMS piezoresistive accelerometers, *Microsystem Technologies,* Vol. 21, Issue 1, 2015, pp. 55-63.

[7]. Yu Xu et al., Analysis and design of a novel piezoresistive accelerometer with axially stressed self-supporting sensing beams *Sensors and Actuators A,* (accepted Manuscript).

[8]. L. A. Rochaa et al., A microinjected 3-axis thermal accelerometer, *Procedia Engineering*, Vol. 25, 2011, pp. 607 - 610.

[9]. Ismail E. Gonenli et al., Surface Micromachined MEMS Accelerometers on Flexible Polyimide

Substrate, *IEEE Sensors Journal*, Vol. 11, Issue 10, 2011, pp. 2318-2325.

[10]. Honglong Chang et al., Design, Fabrication, and Testing of a Bulk Micromachined Inertial Measurement Unit, *Sensors,* Vol. 10, 2010, pp. 3835-3856.

[11]. Serdar Tez et al., A Bulk-Micromachined Three-Axis Capacitive MEMS Accelerometer on a Single Die, *Journal of Micro Electro Mechanical Systems*, Vol. 24, Issue 5, 2015, pp. 1264-1274.

[12]. Chih-ming Sun et al., On the sensitivity improvement of CMOS capacitive accelerometer, *Sensors and Actuators A*, Vol. 141, 2008, pp. 347–352.

[13]. Babak Vakili Amini et al., Micro-gravity capacitive silicon-on-insulator accelerometers, *Journal of Micromechanics and Micro Engineering,* Vol. 15, 2005, pp. 2113–2120.

[14]. Xiaofeng Zhou et al., Design and fabrication of a MEMS capacitive accelerometer with fully symmetrical double-sided H-shaped beam structure, *Microelectronic Engineering*, Vol. 131, 2008, pp. 51-57.

[15]. A. Albarbar et al., Suitability of MEMS accelerometer for condition monitoring: An experimental study, *Sensors,* Vol. 8, Issue 2, 2008, pp. 784–799.

[16]. C.-M. Sun et. al., Implementation of a monolithic single proof-mass tri-axis accelerometer using CMOS-MEMS technique, *IEEE Trans. Electron Devices*, Vol. 57, Issue7, 2010, pp. 1670–1679.

[17]. Ming-Han Tsai et al., A Three-Axis CMOS-MEMS Accelerometer Structure with Vertically Integrated Fully Differential Sensing Electrodes, *Journal of*

Micro Electro Mechanical Systems, Vol. 2, Issue 16, 2012, pp. 329-1337.

[18]. M. S. Khan et al., Physical Level Simulation of Poly MUMPs Based Monolithic Tri-Axis MEMS Capacitive Accelerometer Using FEM Technique, *Advanced Materials Research,* Vol. 403, 2012, pp. 4625-4632.

[19]. F. Mohd-Yasin, et al., Noise and reliability measurement of a three-axis micro-accelerometer, *Microelectronic Engineering*, Vol. 86, 2009, pp. 991–995.

[20]. Sambuddha Khan et al., Improving the Sensitivity and Bandwidth of In-Plane Capacitive Micro Accelerometers Using Compliant Mechanical Amplifiers, *Journal of Micro Electro Mechanical Systems*, Vol. 23, Issue 4, 2014, pp. 871-886.

[21]. Adel Merdassi et al., Wafer level vacuum encapsulated tri-axial accelerometer with lowcross-axis sensitivity in a commercial MEMS Process, *Sensors and Actuators A*, Vol. 236, 2015, pp. 25–37.

[22]. Jiankun Wang et al., Silicon-on-insulator out-of-plane electrostatic actuator with in situ capacitive position sensing, *J. Micro/Nanolith. MEMS MOEMS,* Vol. 11, Issue 3, 2012, pp. 1-8.

[23]. Chang Liu, Foundation of MEMS, Second Edition, *Pearson Publication*, 2012.

[24]. Mark Walter, Jim Carter, Allen Cowen and Greg Hames, SOIMUMPs Design Handbook, *MEMSCAP*, Rev. 2.0, 2002.

[25]. Micro System Analyzer MSA-400. A., *Polytec PI*, Theory, Manual and Software.
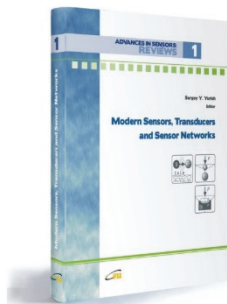
_____

International Frequency Sensor Association (IFSA) Publishing

ADVANCES IN SENSORS: REVIEWS 1

Modern Sensors, Transducers and Sensor Networks

Sergey Y. Yurish, Editor

Modern Sensors, Transducers and Sensor Networks is the first book from the Advances in Sensors: Reviews book Series contains dozen collected sensor related state-of-the-art reviews written by 31 internationally recognized experts from academia and industry.

Built upon the series Advances in Sensors: Reviews - a premier sensor review source, the *Modern Sensors, Transducers and Sensor Networks* presents an overview of highlights in the field. Coverage includes current developments in sensing nanomaterials, technologies, MEMS sensor design, synthesis, modeling and applications of sensors, transducers and wireless sensor networks, signal detection and advanced signal processing, as well as new sensing principles and methods of measurements.

Modern Sensors, Transducers and Sensor Networks is intended for anyone who wants to cover a comprehensive range of topics in the field of sensors paradigms and developments. It provides guidance for technology solution developers from academia, research institutions, and industry, providing them with a broader perspective of sensor science and industry.

Formats: printable pdf (Acrobat) and print (hardcover), 422 pages

ISBN: 978-84-615-9613-3,
e-ISBN: 978-84-615-9012-4

http://sensorsportal.com/HTML/BOOKSTORE/Advance_in_Sensors.htm